Enhanced luminescence in co-doped LaCa$_4$O(BO$_3$)$_3$ phosphor: Photoluminescence, mechanoluminescence and thermoluminescence study

G.C. Mishra [a], Upendra K. Verma [a,*], Ram Sevak Singh [a], S.J. Dhoble [b]

[a] *Department of Physics, OP Jindal University, Raigarh 496001, India*
[b] *Department of Physics, R.T.M. Nagpur University, Nagpur 443300, India*

A B S T R A C T

Mechanoluminescence (ML), Thermoluminescence (TL) and Photoluminescence (PL) characterisation of γ exposed LaCa$_4$O(BO$_3$)$_3$:Cu and LaCa$_4$O(BO$_3$)$_3$:Cu, Mg are studied and synthesised by solid-state reaction process. The phase clarity, crystallinity and configuration of the material is established by XRD while FTIR spectrum of the sample confirms its functional group (BO$_3$)$_3$ and phonon frequency of the molecules in the host. B-O triangle structure defines its constructional inflexibility. SEM characterisation shows particle size of the sample in the micro range and average crystallite size and improvement in the particle size is observed when sample LaCa$_4$O (BO$_3$)$_3$:Cu is mixed with Mg^{2+}. Improvement on the ML, TL and PL peaks are observed on co-doped samples suggest that Mg transfer its energy to Cu ion. The prepared mix borate may be important for optical need due to improvement in the power of the assimilation band and sensorial applications as it respond linearly to γ- ray dose.

1. Introduction

Nonlinear device (NLO) is a significant aspect of everyday life. The light propagates via empty space, and also through material substance, and gives us visual information in relation to the universe. The theory of nonlinear optics builds on the theory of linear optics, known as the interaction of light and matter. The numerous areas of research, such as spectroscopy, semiconductor analysis, photochemistry and sensors have the need of a tuneable sound source of high-energy radiation. The properties of second-order nonlinear ocular coefficient of inorganic crystal LaCa$_4$O(BO$_3$)$_3$ ($d_{12} = 0.26 \pm 0.04$; $d_{32} = 1.69 \pm 0.17$; $d_{eff} = 0.52 \pm 0.05$) and wide transparency wave length range make this phosphor as a potential candidate for nonlinear industry [1–8]. This oxoborate material belongs to monoclinic with space group Cm and possesses a wide transmission range from UV to IR, which is good for NLO applications [9].

At present, researcher focuses on preparing phosphors doping with transition metal due to predominant intensity than rare earth doped samples. Cu$^+$ is one of the key metal activator with transition 3d^{9}4 s^1 ↔3d^{10} and exhibits broad light emission in UV to visible range in an appropriate host. Most of the Cu$^+$ doped host like Na$_2$Zn(PO$_4$)Cl [10], Li$_2$B$_4$O$_7$ [11,12], BaB$_2$O$_4$ [13], Li$_2$NaBF$_6$ [14], Li$_2$BPO$_5$ [15] are studied only for the Photoluminescence characterisation.

Many researchers observed the improvement in the emanation strength of co-doped host phosphors like $ZnWO_4$ (Tm^{3+}, Yb^{3+}, Mg^{2+}), La_2O_3(Zn^{2+}/Mg^{2+}), Li_2SO_4 (Cu/Mg, Cu/P), $Mg_2Al_4Si_5O_{18}$ (Ce/Mn, Ce/Tb), $BaMg_2Al_6Si_9O_{30}$ (Eu, Tb, Mn), $Sr_{3.5}Y_{6.5}O_2$(PO_4)$_{1.5}$(SiO_4)$_{4.5}$: Ce^{3+}/Tb^{3+}/ Mn^{2+} and more [16–21].

The supremacy of nuclear technology in different domains like radiation medicine, non-destructive field, radiotherapy and food processing promote researchers to study new and high-performance TLD materials for dosimetry used. The TL studies of borate compounds like BaB_4O_7: Dy, $Li_2B_4O_7$:Cu, In, $SrBaB_4O_7$:Dy, MgB_4O_7: Dy,Na, $Ba_2Ca(BO_3)_2$:Tb, Sr_2Mg $(BO_3)_2$ are attractive because of their near tissue-equivalent amalgamation coefficient and have been reported as good TL materials [22–27]. A new series of calcium-containing rare-earth oxyborates have been synthesised showed is in structural with the composition of $LnCa_4O(BO_3)_3$ (Ln = La, Sm, Nd, Gd, Er, Y) and has space group monoclinic, non-centrosymmetric. These phosphors exhibit good thermal and chemical stability [28].

Some of the TL materials also show prominent ML peak [29], this fact motivates us for the ML characterisation. Phosphor shows ML intensity by any mechanical means like grinding, cleaving or scratching. The Large number of researchers especially in India, China and Japan are engaged in developing stress sensing techniques [30–34].

Not sufficient work has been observed for the mechanoluminescence (ML) and thermoluminescence (TL) study of co-doped $LaCa_4O$ $(BO_3)_3$: phosphor. In the present article, we have reported PL, TL and ML characterisation of co-doped (Cu/Mg) $LaCa_4O(BO_3)_3$ phosphors amalgamated by solid-state result method. Enhancement in TL, ML and PL peaks of co-doped phosphor samples are explained in this current work.

2. Experimental method

2.1. Amalgamation

$LaCa_4O(BO_3)_3$:Cu, $LaCa_4O(BO_3)_3$:Cu,Mg samples are arranged by solid-state reaction method at high temperature. For synthesis of $LaCa_4O(BO_3)_3$: Cu, Mg, raw materials are Lanthanum oxide (monohydrate), Calcium Carbonate, Boric Acid, (all are A.R., Himedia), Cupric Oxide, Magnesium Carbonate (97% Extra Pure, LOBA). A stoichiometric ratio of all the raw materials were beached systematically followed by heat at around 750 °C intended for 10 h and after that frozen gradually Again these samples were grounded and fired at 850 °C for another 10 h then cooled. The same process was repeated with different concentrations (0.05,0.1,0.2,0.5,1.0 mol%) of dopant Cu separately and then with co-doping (Cu/Mg). The basic chemical reaction is:

$8CaCO_3 + 6 H_3BO_3 + La_2O_3 \rightarrow 2LaCa_4O(BO_3)_3 + 9 H_2O + 8CO_2$
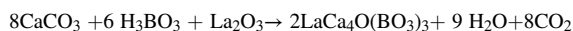
Dopant used: CuO, $MgCO_3$.

2.2. Categorisation

To check the XRD patterns of the $LaCa_4O(BO_3)_3$ with the slandered pattern, an X-ray diffractometer (PW-1710) was used to record X-ray diffraction. A spectrofluorometer is used to measure the photoluminescence (PL) of the doped samples (Maruteck-FL-100-HS). The TL glow curve is recorded using a PC-based TL analyser device (TL-1009I). By dumping a load on a sample mounted on a Lucite plate with varying impact velocities, ML is stimulated spontaneously. A 931 A photomultiplier tube is positioned below the Lucite plate and connected to a storage oscilloscope to monitor the luminescence (SM-340).
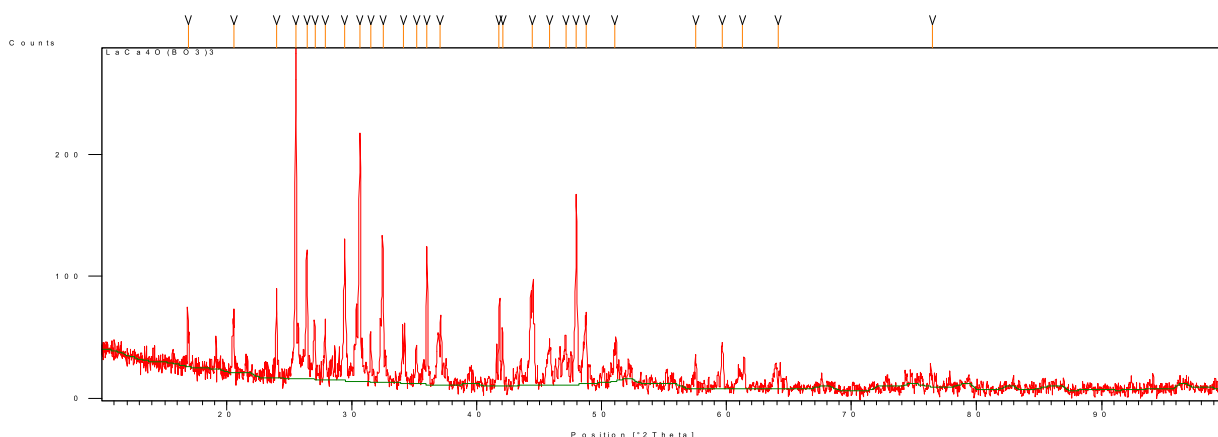

Fig. 1. XRD pattern of $LaCa_4O(BO_3)_3$ crystal.

3. Result and examination

3.1. XRD analysis

The condition of clarity & crystallinity of the sample crystal LaCa$_4$O(BO$_3$)$_3$ was examined by XRD (Fig. 1) and the pattern reveal that all the diffraction peaks (d spacing shown in Chart 1) can be well indexed to the simulated XRD pattern of standard XRD data of LaCa$_4$O(BO$_3$)$_3$ (JCPDS No. 52-0621).

3.2. SEM measurements

The SEM images of Cu and Cu/Mg co-doped LaCa$_4$O(BO$_3$)$_3$ phosphors with different resolution are revealed in Fig. 2.(a) (b). It is illustrated that bit volume is irregular and average crystallite size are in the sub micrometre range because particle morphology is destroyed due to grinding. The particles are seeming to be aggregated to each other during synthesis. We observed enhancement in the particle size when sample LaCa$_4$O(BO$_3$)$_3$:Cu is mixed with Mg^{2+} reported by several groups [16,35,36].

3.3. FTIR measurements

Fig. 3 shows the FTIR spectra of LaCa$_4$O(BO$_3$)$_3$. BO$_3$ groups serve as the central structural units in B-O triangles in the crystal structure of LaCa$_4$O(BO$_3$)$_3$, which provides structural rigidity to the materials. The luminescence properties of the materials are highly influenced by non-bonded oxygen ions (non-bridging oxygen ions). There are four fundamental vibrational modes in the (BO$_3$)$_3$ group. Due to contaminants, the bands above 1500 cm-1 are O-H stretching vibrations. The bands in the 1200–1450 cm-1 range are produced by asymmetric stretching modes of (BO$_3$), whereas bands in the 900–1060 cm-1 range are caused by symmetric stretching modes of (BO$_3$) (BO$_3$). Asymmetric and symmetric bending modes of (BO$_3$), on the other hand, are found in the 650–800 cm-1 and 540–680 cm-1 ranges, respectively.

Pos. [°2Th.]	Height [cts]	FWHM [°2Th.]	d-spacing [Å]	Rel. Int. [%]
16.8547	20.60	0.4896	5.25602	7.52
20.5170	41.37	0.2448	4.32536	15.11
23.9520	60.04	0.1224	3.71224	21.93
25.4982	273.83	0.1428	3.49054	100.00
26.3731	106.33	0.1428	3.37669	38.83
27.0202	44.68	0.1632	3.29728	16.31
27.8394	35.06	0.2448	3.20208	12.80
29.4292	116.73	0.1428	3.03262	42.63
30.6566	200.13	0.1428	2.91395	73.09
31.5063	40.41	0.1632	2.83726	14.76
32.4660	118.35	0.1224	2.75555	43.22
34.1452	25.05	0.3264	2.62378	9.15
35.1515	26.97	0.2448	2.55094	9.85
36.0060	112.68	0.1632	2.49234	41.15

Chart 1. Peak catalogue.
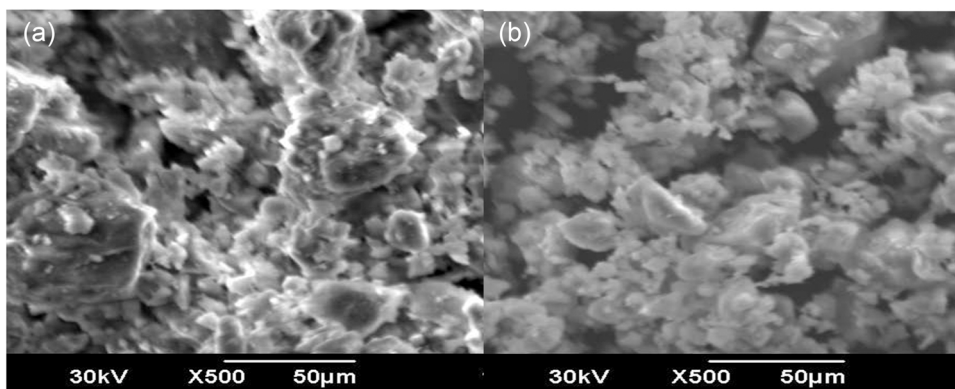
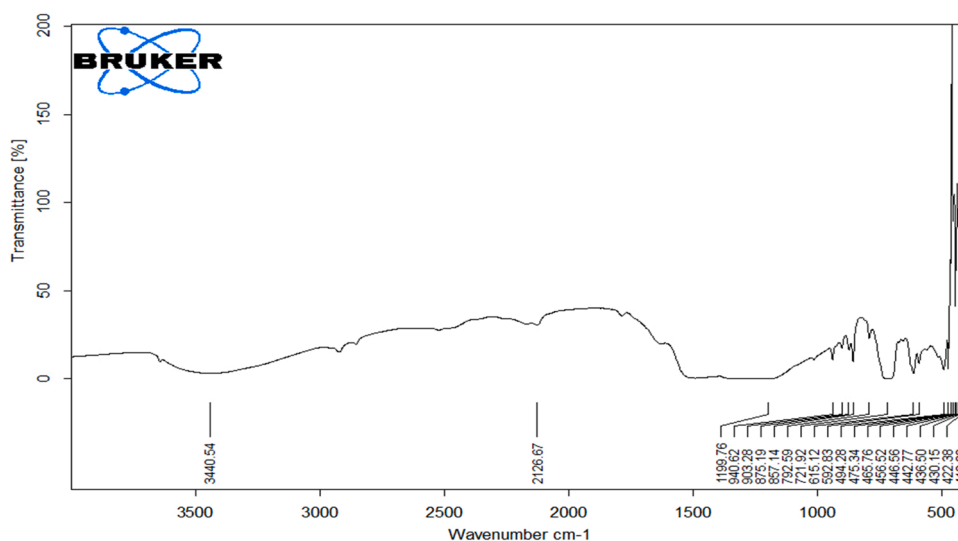**Fig. 2.** (a) SEM images of Cu doped LaCa$_4$O(BO$_3$)$_3$, 2 (b) SEM images Cu/Mg co-doped LaCa$_4$O(BO$_3$)$_3$.

Fig. 3. FTIR spectra of LaCa$_4$O(BO$_3$)$_3$.

External vibrations caused by vibrational and translational movement of (BO$_3$)$_3$, non-bridging oxygen atoms, and translational motions of RE^{3+} and Ca^{2+} ions are shown by the bands below 500 cm^{-1}. The band appeared at 418.13 cm^{-1} in our case is consistent with the band at 418 cm^{-1} of non-bridging oxygen ions reported by Maczka et al. [37,38].
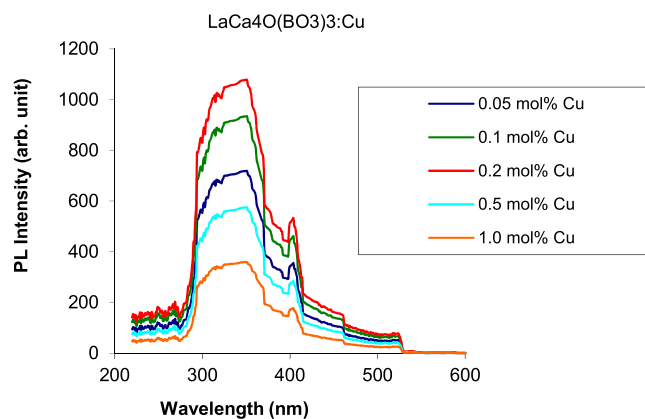

Fig. 4. PL emission spectrum of LaCa$_4$O(BO$_3$)$_3$ with different mol% of Cu.

3.4. Photoluminescence (PL) characterisation

The PL emission spectrum of $LaCa_4O(BO_3)_3$: Cu exhibit a broad band between 300 and 550 nm (Fig. 4). Figure display the emission spectra of the phosphor samples for Cu concentration of 0.05,0.1,0.2,0.5 and 1.0 mol% with excitation at 247 nm wavelength. All the emission peaks with very strong concentrations have dual bump detected by 351 nm with 404 nm assigned to the $3d^9 4 s^1$ $\leftrightarrow 3d^{10}$ transition in Cu^+ ions. The oozing spectra do not change with dopant attentiveness but outstanding transforms seen in the intensity and quenching occurs at 0.2 mol%. It may be due to complex formation; energy transfer or collision in the ground state [39, 40].

The emission intensity of the 0.2 mol% $LaCa_4O(BO_3)_3$:Cu is improved when it is co-doped with Mg(0.05,0.1,0.2,0.5 mol%) at 247 nm excitation (Fig. 5). It seems that energy may move from Mg ions to Cu ions due to the excitation energy provided from Cu to Mg and Cu returns to the ground state. The excited Mg ions then make a downward transition after emitting more photons of greater intensity. It takes place because on adding Mg ion to $LaCa_4O(BO_3)_3$:Cu results in the increase of unit range of the sample and as well improves the power of the assimilation band [16].

3.5. Mechanoluminescence (ML) characterisation

ML strength against time curve of γ-irradiated $LaCa_4O(BO_3)_3$:Cu (0.05,0.1,0.2,0.5,1.0 mol%) and $LaCa_4O(BO_3)_3$:$Cu_{0.2\ mol\%}$,Mg (0.05,0.1,0.2,0.5 mol%) phosphors with different doses (0.5–10 kGy) show a single prominent peak when load of mass 0.6 kg drop on to the prepared samples placed in a lucite plate (Fig. 6(a)(b)). ML intensity improves in the co-doped sample and is maximum for $LaCa_4O(BO_3)_3$:$Cu_{0.2\ mol\%}$,$Mg_{0.1\ mol\%}$. Fig. 7 illustrates the gamma quantity reliance of ML of $LaCa_4O(BO_3)_3$:$Cu_{0.2\ mol\%}$,$Mg_{0.1\ mol\%}$ phosphor. An almost linear increase in ML intensities is observed when gamma-rays are given to a sample.

Like thermal energy, energy can't be passed on to them at bay charge carriers directly; so, some intermediary states square measure answerable for cc emission during this system. one amongst the explanations used for cc emission is piezo-electrification of the crystal throughout the application of load that is exhibited by non-centrosymmetric crystal [41]. The lanthanum oxoborate is a material with a non-centrosymmetric structure [42]. When mechanical strain is applied to the sample, a potential difference is generated due to the accumulation of electric charge. Piezoelectric materials, a subset of ferroelectric materials, exhibit the formation of a local charge separation known as electrical dipoles due to their non-centrosymmetric crystal structure. In the gift investigation, the emission of cubic centimetre is perhaps because of the extreme field, elicited by the electrical dipole throughout the fracture of the sample. The electric field created could result the bending of the conductivity band, pelmet band and trappings centres close to the charged surface, the conductivity band, pelmet band and hole trappings levels can bend downwards; but, close to the charged surface these bands can bend upwards. The numerous band bending could cause tunnelling of the lepton from the pelmet band to the opening trappings centres. Therefore, at intervals an exact depth close to the surface, all the unfree holes could also be free and consequently, they'll be transferred to the framework band & Mg develop the intensity of $LaCa_4O(BO_3)_3$:Cu as Cu ions entrust their energy to Mg ions [43,44].

3.6. Thermoluminescence (TL) characterisation

Fig. 8(a)(b) display a TL glow curves for γ-irradiated $LaCa_4O(BO_3)_3$:Cu (0.05,0.1,0.2,0.5,1.0 mol%) and $LaCa_4O(BO_3)_3$:$Cu_{0.2\ mol\%}$, Mg(0.05,0.1,0.2,0.5 mol%) phosphors with different doses (0.5–10 kGy) at a temperature rate 2 ℃/s which depict a single prominent peak at 180 ℃ for Cu doping and 190 ℃ for co doping of Cu/Mg to the host $LaCa_4O(BO_3)_3$ phosphors. Maximum intensity observed for 0.2 mol% of Cu and then quenching occur for higher concentration. A single glow peak indicates about the formation of one kind of trapping centre due to gamma exposure.

TL glow curve for $LaCa_4O(BO_3)_3$:$Cu_{0.2\ mol\%}$,Mg is observed good for 0.1 mol% of Mg so further experiment is repeated with higher dose for $LaCa_4O(BO_3)_3$:$Cu_{0.2\ mol\%}$,$Mg_{0.1\ mol\%}$ sample and linear dose response is noted (Fig. 9). Linear response is due to formation of more trapping centre with higher doping. Experimentally it is seen that the TL intensity of $LaCa_4O(BO_3)_3$:$Cu_{0.2\ mol\%}$ is less than $LaCa_4O$

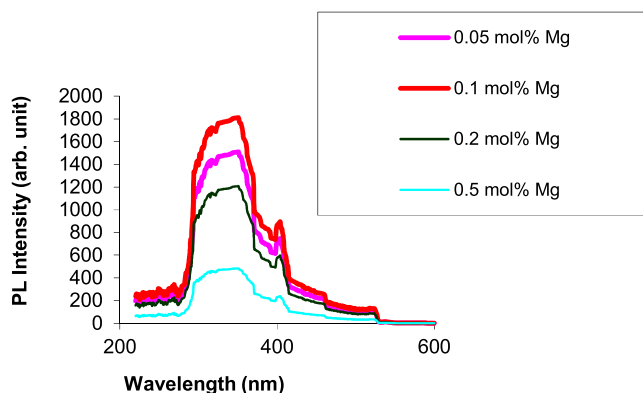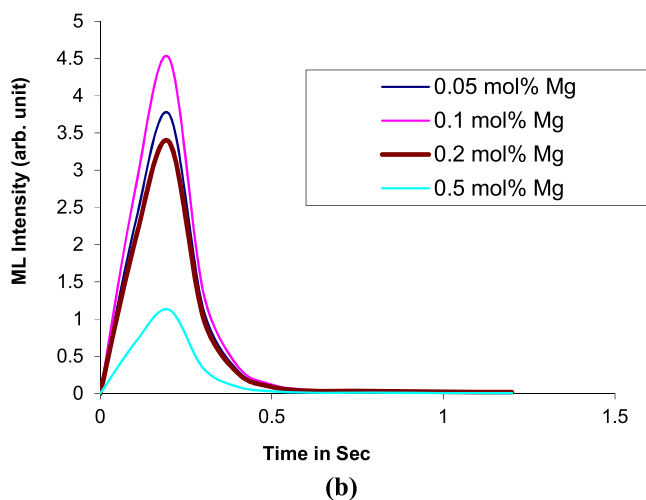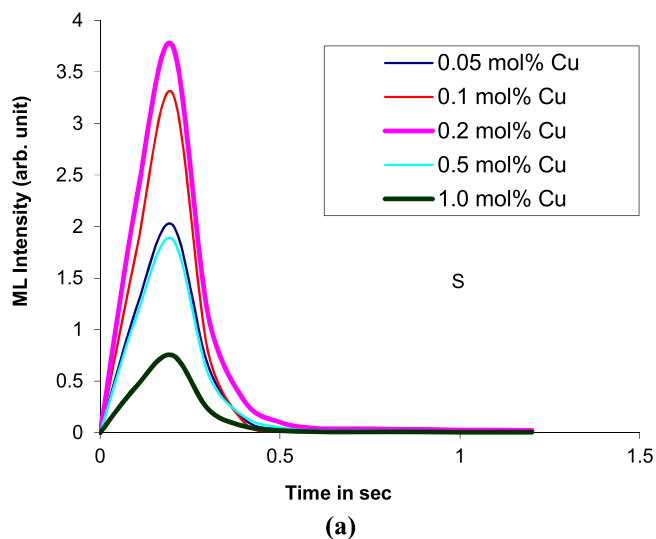**Fig. 5.** PL emission spectrum of $LaCa_4O(BO_3)_3$: $Cu_{0.2\ mol\%}$ with different mol% of Mg.

Fig. 6. (a) ML glow curve of $LaCa_4O(BO_3)_3$ with different mol% of Cu (γ-dose 4 kGy & load of the piston 0.6Kg). (b) ML glow curve of $LaCa_4O$ $(BO_3)_3$: $Cu_{0.2\ mol\%}$ with different mol% of Mg (γ-dose 4 kGy & load of the piston 0.6Kg).
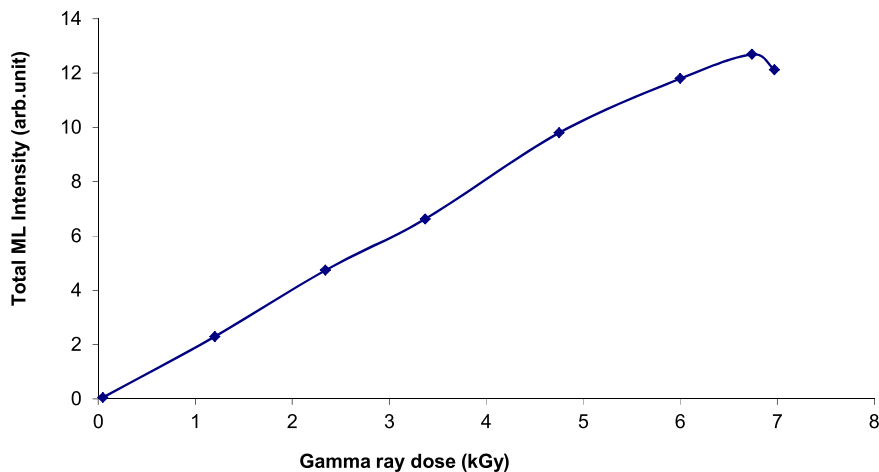
Fig. 7. Total ML Intensity as a function of γ-dose given to $LaCa_4O(BO_3)_3$:$Cu_{0.2\ mol\%}$,$Mg_{0.1\ mol\%}$ phosphor (load of the piston 0.6Kg).
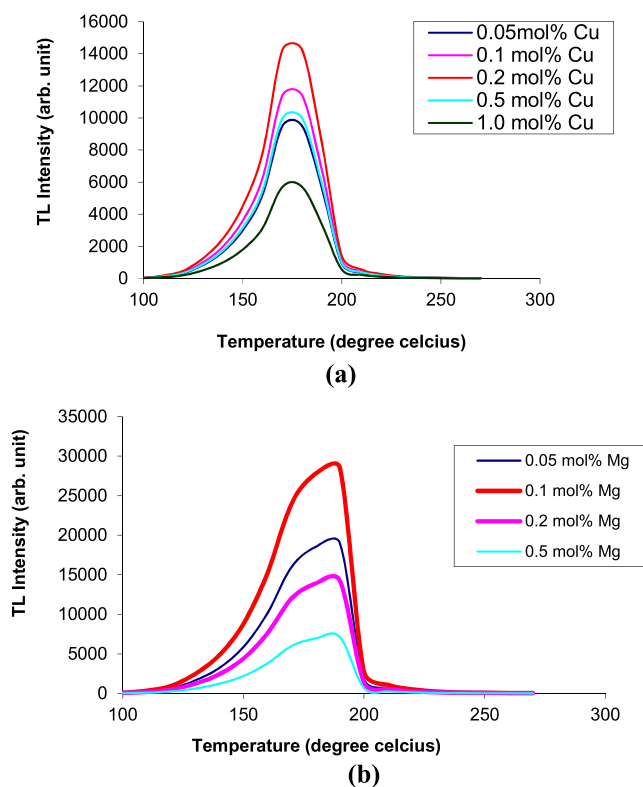
Fig. 8. (a) TL glow curve of LaCa$_4$O(BO$_3$)$_3$ with different mol% of Cu (γ-dose 4 kGy). (b) TL glow curve of LaCa$_4$O(BO$_3$)$_3$:Cu$_{0.2\ mol\%}$ with different mol% of Mg (γ-dose 4 kGy).
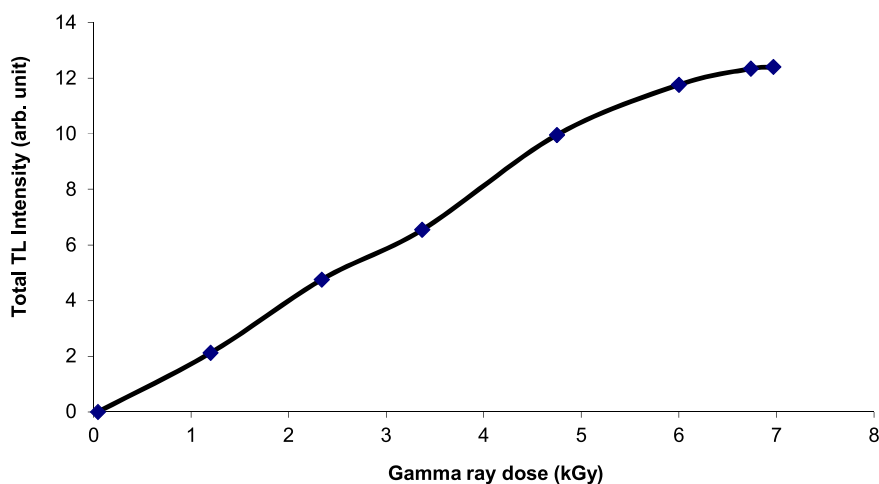

Fig. 9. Total TL Intensity as a function of γ-dose given to LaCa$_4$O(BO$_3$)$_3$:Cu$_{0.2\ mol\%}$,Mg$_{0.1\ mol\%}$ phosphor.

(BO$_3$)$_3$:Cu$_{0.2\ mol\%}$,Mg$_{0.1\ mol\%}$shows that Mg play vital role in the TL secretion due to energy transmit from Cu(sensitizer) to Mg(activator) [44].

4. Conclusion

LaCa$_4$O(BO$_3$)$_3$: Cu, LaCa$_4$O(BO$_3$)$_3$: Cu, Mg phosphors have been synthesised for different concentrations of dopants (Cu/Mg) by solid-state reaction technique and purity and crystallinity is confirmed by XRD of the material. Enhancement in the particle size is observed by SEM when sample LaCa$_4$O (BO$_3$)$_3$:Cu is mixed with Mg^{2+}. FTIR measurement shows that LaCa$_4$O(BO$_3$)$_3$ has BO$_3$ groups as

the essential structural components in B-O triangles which provides constructional inflexibility of the substance. Non-bonded oxygen ions (non-bridging oxygen ions) strongly affect the luminescence properties of the material. ML, TL and PL study shows that the emission intensity of $LaCa_4O(BO_3)_3$: Cu phosphor increases with the presence of Mg ions. Thus, $LaCa_4O(BO_3)_3$: Cu, Mg lanthanum oxoborate may be important for optical and sensorial applications. The material with an associate degree increased ML& TL property shows high potential to be used in period pressure mapping systems, sensible detector networks, high-level security systems, and computer science. It means, it has good market application prospects.

Declaration of Competing Interest

The authors declare that they have no known competing financial interests or personal relationships that could have appeared to influence the work reported in this paper.

References

[1] R.C. Miller, W.A. Nordland, K. Nassau, Nonlinear optical properties of Gd2(MoO4)3 and Tb2 (MoO4)3, Ferroelectrics 2 (1971) 97, https://doi.org/10.1080/00150197108241497.

[2] Marie Münchhalfen, J.ürgen Schreuer, Christoph Reuther, Erik Mehner, Hartmut Stöcker, Elastic, piezoelectric, and dielectric properties of rare-earth calcium oxoborates RCa4O(BO3)3 (R = Er, Y, Dy, Gd, Sm, Nd, La), J. Appl. Phys. 130 (2021), 095102, https://doi.org/10.1063/5.0061747.

[3] R.C. Miller, W.A. Nordland, Absolute signs of second harmonic generation coefficients of piezoelectric crystals, Phys. Rev. B 2 (1970) 4896, https://doi.org/10.1103/PhysRevB.2.4896.

[4] S. Singh, Nonlinear optical properties, in: M.J. Weber (Ed.), Handbook of Laser Science and Technology, Vol. III Optical Materials, CRC Press, Inc., Boca Raton, 1986, https://doi.org/10.1201/9781003067955.

[5] J.J. Adams, C.A. Ebbers, K.I. Schaffers, S.A. Payne, Nonlinear optical properties of LaCa4O(BO3)3, Opt. Lett. 26 (2001) 217, https://doi.org/10.1364/OL.26.000217.

[6] V.G. Dmitriev, G.G. Gurzadyn, D.N. Nikogosyan, Handbook of Nonlinear Optical Crystals, Springer-Verlag, New York, 1991, https://doi.org/10.1002/crat.2170290511.

[7] Yi. Lu Hu Z., Z. Lin, G. Wang, Growth and spectroscopic properties of Er3+/Yb3+:LaCa4O(BO3)3 crystals, J. Cryst. Growth 249 (2003) 159–162, https://doi.org/10.1016/S0022-0248(02)01992-9.

[8] H.J. Zhang, H.D. Jiang, J.Y. Wang, X.B. Hu, G.W. Yu, W.T. Yu, L. Gao, J.A. Liu, S.J. Zhang, M.H. Jiang, Growth and characterization of a LaCa4O(BO3)3 crystal, Appl. Phys. A 78 (2004) 889–893, https://doi.org/10.1007/s00339-003-2085-9.

[9] H. Jiang, Da Wei Li, K. Zhang, H. Liu, Ji Yang Wang, Optical and thermal properties of nonlinear optical crystal LaCa4O (BO3)3, Chem. Phys. Lett. 372 (2003) 788–793, https://doi.org/10.1016/S0009-2614(03)00508-6.

[10] V. Yerpude, S. Tamboli, K.B. Ghormare, S.J. Dhoble, Optical properties of Cu+ ions activated Na2Zn(PO4)Cl phosphor, J. Optoelectron. Adv. Mater. 20 (2018) 651–656.

[11] G.D. Patra, M. Tyagi, D.G. Desai, B. Tiwari, S. Sen, S.C. Gadkari, Photo-luminescence properties of Cu and Ag doped Li2B4O7 single crystals at low temperatures, J. Lumin. 132 (2012) 1101–1105, https://doi.org/10.1016/j.jlumin.2011.12.005.

[12] G.D. Patra, S.G. Singh, B. Tiwari, S. Sen, D.G. Desai, S.C. Gadkari, Thermally stimulated luminescence process in copper and silver codoped lithium tetraborate single crystals and its implication to dosimetry, J. Lumin. 137 (2013) 28–31, https://doi.org/10.1016/j.jlumin.2012.12.007.

[13] N. Liu, Y. Tian, L. Yu, Q. Li, F. Meng, Y. Zheng, G. Zhang, Z. Liu, J. Li, F. Jiang, Synthesis and surface modification of uniform barium borate nanorods for lubrication, J. Alloy. Compd. 466 (2008) L11–L14, https://doi.org/10.1016/j.jallcom.2007.11.053.

[14] S.P. Puppalwar, S.J. Dhoble, N.S. Dhoble, Animesh Kumar, Luminescence characteristics of Li2NaBF6: Cu phosphor, Nucl. Instrum. Methods Phys. Res. Sect. B Beam Interact. Mater. At. 274 (2012) 167–171, https://doi.org/10.1016/j.nimb.2011.10.012.

[15] S.P. Puppalwar, S.J. Dhoble, Animesh Kumar, Cu+ emission in Li2BPO5 material for thermoluminescence dosimetry, Radiat. Eff. Defect Solids 167 (2012) 333–334, https://doi.org/10.1080/10420150.2011.653663.

[16] R.S. Yadav, S.J. Dhoble, S.B. Rai, Enhanced photoluminescence in Tm3+, Yb3+, Mg2+ tri doped ZnWO4 phosphor: three photon upconversion, laser induced optical heating and temperature sensing, Sens. Actuators B Chem. 273 (2018) 1425–1434, https://doi.org/10.1016/j.snb.2018.07.049.

[17] A. Kumari, A. Pandey, R. Dey, V.K. Rai, Simultaneous influence of Zn2+/Mg2+ on the luminescent behaviour of La2O3: Tm3+-Yb3+ phosphors, RSC Adv. 4 (2014) 21844–21851, https://doi.org/10.1039/C4RA01400F.

[18] S.P. Puppalwar, S.J. Dhoble, Animesh Kumar, Improvement of photoluminescence of Cu+ ion in Li2SO4, Lumin. Biol. Chem. Lumin. 26 (2011) 456–461, https://doi.org/10.1002/bio.1252.

[19] Wei Lu, Y. Jia, W. Lv, Qi Zhao, H. You, Energy transfer studies of Ce3+-Mn2+ and Ce3+-Tb3+ in an emitting tunable Mg2Al4Si5O18: Ce3+/Mn2+/Tb3+ phosphor, Opt. Mater. 42 (2015) 62–66, https://doi.org/10.1016/j.optmat.2014.12.019.

[20] W. Lu, Z.D. Hao, X. Zhang, Y.S. Luo, X.J. Wang, J.H. Zhang, Inorg. Chem., No. 50 (2011) 7846.

[21] Haikun Liu, Yi Luo, Zhiyong Mao, Libing Liao, Zhiguo Xia, A novel single-composition trichromatic white emitting Sr3.5Y6.5O2(PO4)1.5(SiO4)4.5:Ce3+/Tb3+/Mn2+ phosphor: synthesis, luminescent properties and applications for white LEDs, J. Mater. Chem. C 2 (2014) 1619–1627, https://doi.org/10.1039/C3TC32003K.

[22] J. Li, J.Q. Hao, C.X. Zhang, Q. Tang, Y.L. Zhang, Q. Su, S. Wang, Thermoluminescence characteristics of BaB4O7:Dy phosphor, Nucl. Instrum. Methods Phys. Res. B Beam Interact. Mater. At. 222 (2004) 577, https://doi.org/10.1016/j.nimb.2004.03.005.

[23] C. Furetta, M. Prokic, R. Salamon, V. Prokic, G. Kitis, Dosimetric characteristics of tissue equivalent thermoluminescent solid TL detectors based on lithium borate, Nucl. Instrum. Methods Phys. Res. Sect. A Accel. Spectrom. Detect Assoc. Equip. 456 (2001) 411–417, https://doi.org/10.1016/S0168-9002(00)00585-4.

[24] J. Li, J.Q. Hao, C.Y. Li, C.X. Zhang, Q. Tang, Y.L. Zhang, Q. Su, S.B. Wang, Thermally stimulated luminescence studies for dysprosium doped strontium tetraborate, Radiat. Meas. 39 (2005) 229–233, https://doi.org/10.1016/j.radmeas.2004.06.006.

[25] C. Furetta, G. Kitis, P.S. Weng, T.C. Chu, Thermoluminescence characteristics of MgB4O7: Dy, Na, Nucl. Instrum. Methods Phys. Res. Sect. A Accel. Spectrom. Detect. Assoc. Equip. 420 (1999) 441–445, https://doi.org/10.1016/S0168-9002(98)01198-X.

[26] L.Y. Liu, Y.L. Zhang, J.Q. Hao, C.Y. Li, Q. Tang, C.X. Zhang, Q. Su, Thermoluminescence characteristics of terbium-doped Ba2Ca(BO3)2 phosphor, Phys. Status Solidi A 202 (2005) 2800–2806, https://doi.org/10.1002/pssa.200521199.

[27] L.Y. Liu, Y.L. Zhang, J.Q. Hao, C.Y. Li, Q. Tang, C.X. Zhang, Q. Su, Thermoluminescence studies of rare earth doped Sr2Mg(BO3)2 phosphor, Mater. Lett. 60 (2006) 639–642, https://doi.org/10.1016/j.matlet.2005.09.050.

[28] R. Norrestam, J.O. Bovin Nygran, Structural investigations of new calcium rare-earth oxyborates with the composition Ca4RO(BO3)3, Chem. Mater. 4 (1992) 737–743, https://doi.org/10.1021/cm00021a044.

[29] A.K. Upadhyay, S.J. Dhoble, R.S. Kher, Mechanoluminescence of gamma-ray irradiated and Eu activated BaSO4 phosphor was studied Luminescence, J. Biol. Chem. Lumin. 26 (2011) 471–476, https://doi.org/10.1002/bio.1254.

[30] C.N. Xu, T. Watanabe, M. Akiyama, X.G. Zheng, Direct view of stress distribution in solid by mechanoluminescence, Appl. Phys. Lett. 74 (1999) 2414–2416, https://doi.org/10.1063/1.123865.

[31] M. Akiyama, C.N. Xu, M. Taira, K. Nonaka, T. Watanabe, Visualization of stress distribution using mechanoluminescence from Sr3Al2O6: Eu and the nature of the luminescence mechanism, Philos. Mag. Lett. 79 (1999) 735–740, https://doi.org/10.1080/095008399176797.

[32] C.N. Xu, X.G. Zheng, M. Akiyama, K. Nonaka, T. Watanabe, Dynamic visualization of stress distribution by mechanoluminescence image, Appl. Phys. Lett. 76 (2000) 179–181, https://doi.org/10.1063/1.125695.

[33] C. Li, C.N. Xu, H. Yamada, Y. Imai, H. Zhang, L. Zhang, A novel technique for viewing stress distribution with mechanoluminescence materials, Key Eng. Mater. 368 –372 (2008) 1401–1404, https://doi.org/10.4028/www.scientific.net/KEM.368-372.1401.

[34] K.S. Sohn, S.Y. Seo, Y.N. Kwon, H.D. Park, Direct observation of crack tip stress field using the mechanoluminescence of SrAl2O4:(Eu, Dy, Nd), J. Am. Ceram. Soc. 85 (2002) 712–714, https://doi.org/10.1111/j.1151-2916.2002.tb00158.x.

[35] Q. Sun, H. Zhao, X. Chen, F. Wang, W. Zhao, W. Cai, Z. Jiang, Upconversion emission enhancement in silica-coated Gd_2O_3:Tm^{3+}, Yb^{3+} nanocrystals by incorporation of Li^+ ion, Mater. Chem. Phys. 123 (2010) 806–810, https://doi.org/10.1016/j.matchemphys.2010.05.064.

[36] J.H. Chung, S.Y. Lee, K.B. Shim, S.Y. Kweon, S.C. Urand, J.H. Ryu, Blue Upconversion luminescence of CaMoO4:Li/Yb Tm phosphors prepared by complex citrate method, in: Appl. Phys. A, 108, 2012, pp. 369–373, https://doi.org/10.1007/s00339-012-6893-7.

[37] G. Barros, E.N. Silva, A.P. Ayala, I. Guedes, C.K. Loong, J. Wang, X. Hu, H. Zhang, Raman spectroscopic characterization of $RECa_4O(BO_3)_3$ (RE = La and Gd) crystals, Vib. Spectrosc. 46 (2008) 100–106, https://doi.org/10.1016/j.vibspec.2007.11.002.

[38] M. Mączka, J. Hanuza, A. Pajączkowska, Y. Morioka, J.H. van der Maas, Lattice dynamics of $Ca_4GdO(BO_3)_3$, J. Raman Spectrosc. 35 (2004) 266–273, https://doi.org/10.1002/jrs.1146.

[39] D.S. McClure, S.C. Weaver, Electronic spectra and electronic structure of the Cu^+ ion in alkali halides, J. Phys. Chem. Solids 52 (1991) 81–99, https://doi.org/10.1016/0022-3697(91)90061-4.

[40] P.D. Bhoyar, R. Choithrani, S.J. Dhoble, Study of electron-vibrational interaction and concentration quenching effect of Cu+ ions in lithium based sulphate phosphors, Solid State Sci. 57 (2016) 24–32, https://doi.org/10.1016/j.solidstatesciences.2016.05.002.

[41] B.P. Chandra, C.N. Xu, H. Yamada, X.G. Zheng, Luminescence induced by elastic deformation of ZnS:Mn nanophosphors, J. Lumin. 130 (2010) 442–450, https://doi.org/10.1016/j.jlumin.2009.10.010.

[42] C. Reuther, R. Möckel, M. Hengst, J. Götze, A. Schwarzer, H. Schmidt, Growth and structure of Ca4La[O|(BO3)3], Materials Science, J. Cryst. Growth 320 (2011) 90–94, https://doi.org/10.1016/j.jcrysgro.2011.02.007.

[43] B.P. Chandra, Mechanoluminescence', in: D.R. Vij (Ed.), Luminescence of Solids, Plenum Press, New York, 1998, pp. 361–389, https://doi.org/10.1007/978-1-4615-5361-8_10.

[44] P.S. Thakre, S.C. gedam, S.J. Dhoble, Thermoluminescence properties of γ-irradiated KCaSO4Cl:X (X = Ce, Dy, Mn or Pb), J. Mater. Sci. 47 (2012) 1860–1866, https://doi.org/10.1007/s10853-011-5973-y.